ORIGINAL RESEARCH

Novel nanostructured biomaterials: implications for coronary stent thrombosis

Varvara Karagkiozaki[1,2]
Panagiotis G Karagiannidis[1]
Nikolaos Kalfagiannis[1]
Paraskevi Kavatzikidou[1]
Panagiotis Patsalas[3]
Despoina Georgiou[1]
Stergios Logothetidis[1]

[1]Lab for Thin Films – Nanosystems
and Nanometrology (LTFN), Physics
Department, Aristotle University of
Thessaloniki, Thessaloniki, [2]AHEPA
Hospital, Aristotle University
of Thessaloniki, Thessaloniki,
[3]Department of Materials Science and
Engineering, University of Ioannina,
Ioannina, Epirus, Greece

Background: Nanomedicine has the potential to revolutionize medicine and help clinicians to treat cardiovascular disease through the improvement of stents. Advanced nanomaterials and tools for monitoring cell–material interactions will aid in inhibiting stent thrombosis. Although titanium boron nitride (TiBN), titanium diboride, and carbon nanotube (CNT) thin films are emerging materials in the biomaterial field, the effect of their surface properties on platelet adhesion is relatively unexplored.

Objective and methods: In this study, novel nanomaterials made of amorphous carbon, CNTs, titanium diboride, and TiBN were grown by vacuum deposition techniques to assess their role as potential stent coatings. Platelet response towards the nanostructured surfaces of the samples was analyzed in line with their physicochemical properties. As the stent skeleton is formed mainly of stainless steel, this material was used as reference material. Platelet adhesion studies were carried out by atomic force microscopy and scanning electron microscopy observations. A cell viability study was performed to assess the cytocompatibility of all thin film groups for 24 hours with a standard immortalized cell line.

Results: The nanotopographic features of material surface, stoichiometry, and wetting properties were found to be significant factors in dictating platelet behavior and cell viability. The TiBN films with higher nitrogen contents were less thrombogenic compared with the biased carbon films and control. The carbon hybridization in carbon films and hydrophilicity, which were strongly dependent on the deposition process and its parameters, affected the thrombogenicity potential. The hydrophobic CNT materials with high nanoroughness exhibited less hemocompatibility in comparison with the other classes of materials. All the thin film groups exhibited good cytocompatibility, with the surface roughness and surface free energy influencing the viability of cells.

Keywords: platelets, cell viability, titanium boron nitride, atomic force microscopy, carbon nanotubes

Background

A significant issue in the cardiovascular field is the placement of stents into stenotic arteries to restore blood flow perfusion into myocardial tissues without causing acute or late stent thrombosis and restenosis due to neointimal hyperplasia. Although the higher clinical efficacy of angioplasty with stenting, compared with angioplasty, has been supported by randomized trials and clinical studies,[1,2] stent drawbacks such as clotting, malpositioning, mechanical rupture, and restenosis still exist. To address the issue of in-stent restenosis, caused almost exclusively by neointimal tissue, drug-eluting stents were developed. This next generation of stents has elicited antiproliferative drugs

Correspondence: Stergios Logothetidis
Aristotle University of Thessaloniki,
Physics Department, Laboratory for Thin
Films – Nanosystems and Nanometrology
(LTFN), Thessaloniki, GR-54124, Greece
Tel +30 2310 998174
Fax +30 2310 998390
Email logot@auth.gr

leading to a restenosis rate of less than 10% compared with that of bare metal stents (20%–30%).[3]

However, there is some evidence that drug-eluting stents may be susceptible to an event known as "late stent thrombosis," in which the blood clotting inside the stent can occur one or more years post-stenting.[4] Unfortunately, both the eluted drug agents with cytostatic or cytotoxic effects on the proliferation of the smooth muscle cells on the arterial wall, as well as the polymeric stent reservoir for drugs, were found to disrupt the natural healing response of the endothelium. The latter is a living tissue that is antithrombotic, inhibits leukocyte recruitment, and secrets dilatation factors such as nitric oxide and prostaglandin prostacyclin. Consequently, it is essential that the development of a suitable stent material/surface takes into consideration control of its physicochemical properties for enhanced cellular endothelial cell growth. Another significant parameter, in order to minimize stent rejection, is the fact that direct contact between stent and blood may trigger activation of platelets and blood coagulation pathways leading to clot formation on the stent surface and arterial occlusion.[5] Thus, the functionality and performance of the biomaterial should be improved to reduce the risk of platelet aggregation/thromboembolism and any complications following the lifelong treatment with anticoagulants.

Recent research has focused on coronary stent surfaces using nanotechnology strategies.[6,7] Carbon- and titanium-based coatings have attracted much interest due to their good mechanical and biological performance. Until now, carbon coatings have been used for medical implants and titanium-based coatings for medical and surgical tools. Our previous studies on amorphous hydrogenated carbon (a-C:H) thin films with respect to plasma protein adsorption and platelet adhesion have shown good biocompatibility results.[8–10] Thus, in this study, a-C:H films were used as the case study materials and their thrombogenicity and cytocompatibility were compared with the ones of boron nitride (TiBN)-, titanium diboride (TiB$_2$)-, and carbon nanotube (CNT)-based thin films. Although various studies have focused on the mechanical response, optical, and electron transport properties of TiBN films,[11] their hemocompatibility, as correlated to their structural characteristics, has not been extensively investigated.

CNTs have emerged as a new and efficient tool for the transport and translocation of therapeutic molecules. CNTs can be functionalized with bioactive peptides, proteins, nucleic acids, and drugs, and used to deliver their cargos to cells and organs.[12] Because functionalized CNTs are not immunogenic and display low toxicity, they have great potential for use in the nanomedicine field.[13] There is reason for these materials to be further assessed, since different growth techniques result in specific physicochemical material characteristics and specific cell viability behavior. With the same goal in mind, herein, we develop these types of biomaterials with well-defined and tailored properties and assess their feasibility to repel platelets for cardiovascular stent applications.

This work presents original results regarding the thrombogenicity potential of TiBN- and CNT-based thin films compared with a-C:H and stainless steel (SS) reference materials (SS is a contemporary and widely used material for bare metal stents) through the investigation of human platelet adhesion by atomic force microscopy (AFM). To the best of our knowledge, this is the first thrombogenicity study of CNT composites and TiBN made via AFM implementation. Cell viability studies were also performed in parallel to test the safety of these novel nanomaterials.

Methods and materials
a-C:H thin films

The sputtered a-C:H thin films (100 nm thick) studied in this work were deposited by radio frequency magnetron sputtering on silicon substrates at room temperature (RT). Details about the growth of the films have been described elsewhere.[14] For the growth of a-C:H films, hydrogen (H$_2$)-reactive gas was introduced into the vacuum deposition chamber. The energy of the ions (mainly argon [Ar]+ or H+), bombarding the growing film surface were varied by applying a substrate floating bias voltage Vb (+10 V) or a negative Vb (−40 V) for the a-C:H films, in 5% H$_2$ within plasma.

TiBN and titanium diboride (TiB$_2$) thin films

TiB$_x$N$_y$ thin films with a thickness of 100 nm were fabricated employing the magnetron sputtering technique in an unbalanced configuration. A series of films was grown under the same negative substrate bias voltage (Vb = −40 V) varying the nitrogen (N$_2$) flow. The sputtered gas (Ar) pressure was set constant for all the experiments. Table 1 presents the material samples, the deposition techniques with the main growth parameters (eg, substrate bias), and the physicochemical properties. The study of the composition of the TiBN samples was realized by X-ray photoelectron spectroscopy in an ultra high-vacuum chamber (Pb $<$ 10^{-8} Pa) after sputter etching with an Ar ion beam. X-ray photoelectron spectroscopy

Table 1 Materials tested, deposition techniques, main growth parameters, surface nanoroughness, stoichiometry, contact angle, and surface free energy parameters of the samples

Material	Deposition technique	Substrate bias (V)	N_2 flow (sccm)	Surface roughness (nm)	Contact angle (°)	Surface free energy (mN/m)
a-C:H (5% H_2)	MS	Biased (−40)	–	0.3	61	47.2
a-C:H (5% H_2)	MS	Floating	–	2.1	63	46
$TiBN_{0.95}$	Unbalanced MS	Biased (−40)	8	1	94.4	26.5
$TiB_{0.9}N_{0.95}$	Unbalanced MS	Biased (−40)	10	2	92.5	27.7
$TiB_{2.13}$	Unbalanced MS	Biased (−40)	0	0.44	40.2	59.3
CNTs	Thermal CVD	–	–	52.3	160	0.3
Stainless steel	–	–	–	74	–	–

Abbreviations: a-C:H, amorphous hydrogenated carbon thin films; MS, magnetron sputtering; TiBN, titanium boron nitride; TiB_2, titanium diboride; CNTs, carbon nanotube-based thin films; CVD, chemical vapor deposition.

analysis rendered the stoichiometry of the samples, shown comparatively in Table 1.

CNT-based thin films and SS

The CNT samples were grown by thermal chemical vapor deposition using a diamond-like carbon (DLC) with nickel catalytic layer deposited by pulse laser deposition on a silicon substrate. The nickel was then removed using aqua regis to avoid its toxicity and to manufacture nanopores (with pore size < 0.1 μm) for promotion of cell growth. SS was used as reference material.

Characterization of the surface properties of the thin films

AFM measurements were performed with a SOLVER P47H scanning probe microscope (NT-MDT, Moscow, Russia) in an ambient environment using the tapping mode for imaging of the surface of the engineered TiBN, TiB_2, a-C:H, SS, and CNT/DLC nanomaterials. Standard silicon cantilevers with a nominal spring constant of Kc = 1.45–15.1 N/m, resonance frequency 87–230 kHz, and high aspect ratio conical tips with a curvature radius of 10 nm were used. Scanning electron microscopy (SEM) was also implemented for visualization of the CNT/DLC samples.

The surface energy of the thin films was acquired by contact angle (CA) measurements, which were performed with a CAM200 optical CA and surface tension meter (KSV Instruments, Helsinki, Finland) using the sessile drop technique. The liquid used was H_2O, with a drop volume of 5 μL and a surface tension of 72.8 mN/m, and the CAs of each sample were recorded within 5 seconds following placement of droplets onto the thin films. The average CA value was obtained by measuring at five different positions on the same sample. The CAs were converted into surface energy values employing the relation of Chibowski and Perea-Carpio.[15]

Platelet adhesion experiments

Venous blood was drawn from healthy volunteers (who did not take any antiplatelet/antithrombotic drugs) and kept in an anticoagulant with acid citrate tubes. Afterwards, the blood was centrifuged at $4 \times g$ for 7–10 minutes at RT to yield platelet-rich plasma (PRP). The thin films were cleaned with N_2 gas flow then they were incubated in PRP at RT and examined by AFM. The tapping AFM was applied, as this is the optimum mode to avoid soft-platelet destruction.[16] AFM is a type of high-resolution scanning probe microscopy, with a demonstrated resolution of fractions of a nanometer, ideal for the imaging of living biological samples due to its non-destructive performance. The morphology of the adherent platelets was investigated at 1- and 2-hour intervals and root-mean-square roughness (R_{rms}) was used for the evaluation of surface roughness of the bare films and after platelet adhesion, for ten areas chosen at random, to obtain statistical averages of the adherent platelets (using Student's t-test).

Cytotoxicity tests
Cell culture

Before being seeded with the cells, all thin films were washed with ethanol for 5 minutes then dried in air. L929 murine fibroblasts are an immortalized cell line with tolerance properties against demanding surfaces. The cell line was cultured in Medium 199 (Gibco, Life Technologies, Carlsbad, CA), containing 5% fetal bovine serum, ascorbic acid, and gentamicin at 37°C, in a humidified atmosphere of 5% CO_2 in air. For the subculture process, the cell monolayer was washed twice with phosphate-buffered saline and incubated

with trypsin solution (0.05% trypsin) for 5 minutes at 37°C to detach the cells. Following this, the cells were resuspended in culture medium and cultured for 24 hours in standard tissue culture plates and on the thin films. Cultures were evaluated for cell viability/adhesion for 24 hours (3-(4,5-Dimethylthiazol-2-yl)-2,5-diphenyltetrazolium bromide [MTT] assay). For comparison purposes, control samples (standard tissue culture plates) were also prepared.

Cell viability assay: MTT assay

The principle of this assay is that live cells, which are metabolically active, reduce tetrazolium salts to colored formazan compounds. Therefore, the MTT salt is converted to blue/purple formazan by living cells. This was used to measure cell viability/proliferation in our study. The culture medium was removed and cultures were incubated with 0.5 mg/mL of MTT solution (in phosphate-buffered saline) for 4 hours. Subsequently, formazan salts were dissolved with isopropanol and the absorbance (in terms of optical density) was measured at 570 nm in an enzyme-linked immunosorbent assay reader (ELx800, BioTek, Winooski, VT). The reference wavelength of 630 nm was also used to measure the same wells and the optical densities obtained were subtracted from the absorbance

of 570 nm to remove any background noise and culture medium obstructions. The data were then optimized to the control to obtain cell viability and cell viability %.

Statistical analysis

Three samples were used for each group of thin films. The results are shown as the mean ± standard deviation.

Results

Nanoscale surface characterization and wetting properties of carbon- and titanium-based thin films

TiBN and TiB$_2$ films

As nanotopography modulates cell behavior, the AFM technique was applied for topography analysis of the nanomaterials developed in this work. It was found that all TiBN and TiB$_2$ films were ultra smooth, having an R$_{rms}$ below a nanometer (approximately 0.4 nm). This was attributed to the layer-by-layer growth of the biased coatings induced by the kinetic energy of the sputtered atoms during deposition. Figure 1A shows the AFM topography images of the series of biased TiBN coatings.
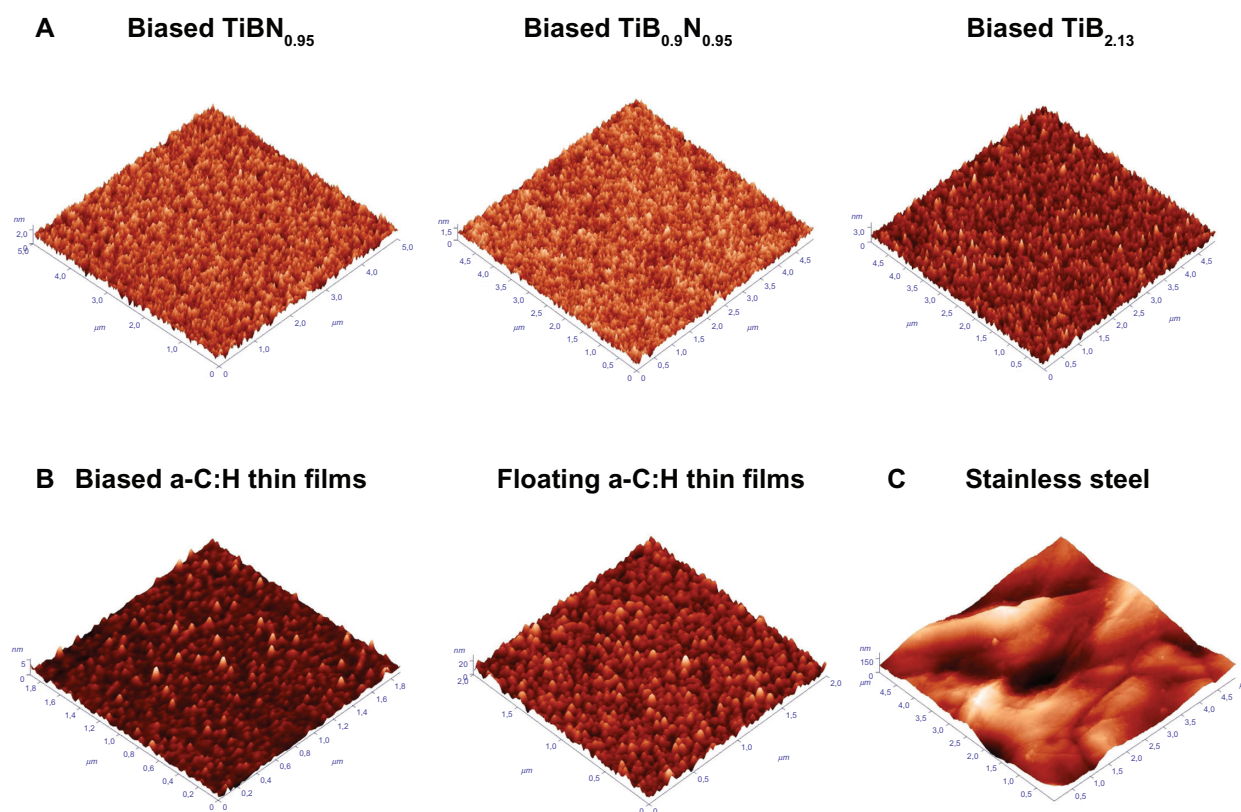
Figure 1 Atomic force microscopy three-dimensional topography images of: (**A**) biased titanium (Ti) boron (B) nitride (N) films (TiBN$_{0.95}$, TiB$_{0.9}$N$_{0.95}$, and TiB$_{2.13}$ films, in sequence); (**B**) carbon thin films (biased and floating amorphous hydrogenated carbon [a-C:H] coatings); and (**C**) stainless steel, as reference material.

Carbon thin films

The biased a-C:H thin films were atomically smooth. In contrast to biased a-C:H thin films, the floating films have higher R_{rms} roughness values (R_{rms} approximately 2.1 nm) as the bias voltage application during deposition (floating conditions) gives the potential to the carbon atoms to form aggregates and islands. Figure 1B shows the a-C:H thin films observed by AFM.

SS and CNT/DLC thin films

SS was found to have a high surface roughness of 74 nm (Figure 1C). The CNT/DLC coatings also had a high surface roughness (R_{rms} approximately 53 nm) due to the presence of the nanotubes. Figure 2A and B show SEM images of the CNT/DLC biomaterial. In particular, Figure 2A shows a cross-section SEM image of the nanotubes on the DLC substrate (the inset shows a cartoon schematic detailing the CNTs deposited onto the DLC) and Figure 2B is an SEM image of the CNTs that shows their spaghetti-like structure. AFM images (Figure 2C and D) revealed that the CNTs were discriminated very well (circled in the figure), having the spaghetti-like form, with the high contrast in phase image (Figure 2D) indicating the formation of nanopores. CA measurements of TiBN, TiB$_2$, CNT/DLC, and a-C:H thin films revealed the differences between the wetting properties of the studied films. The CA of the a-C:H films was, 61°–63°; of the TiBN films was, 92.5°–94.4°; of the TiB2 films was, 40.2°; and of the CNT/DLC films was, 160° (Table 1).

Thrombogenicity assessment and interpretation of the AFM data

Thrombogenesis constitutes a major problem associated with the clinical use of all kinds of prosthetics. Thus, in this study, platelet interactions with the selected biomaterials were
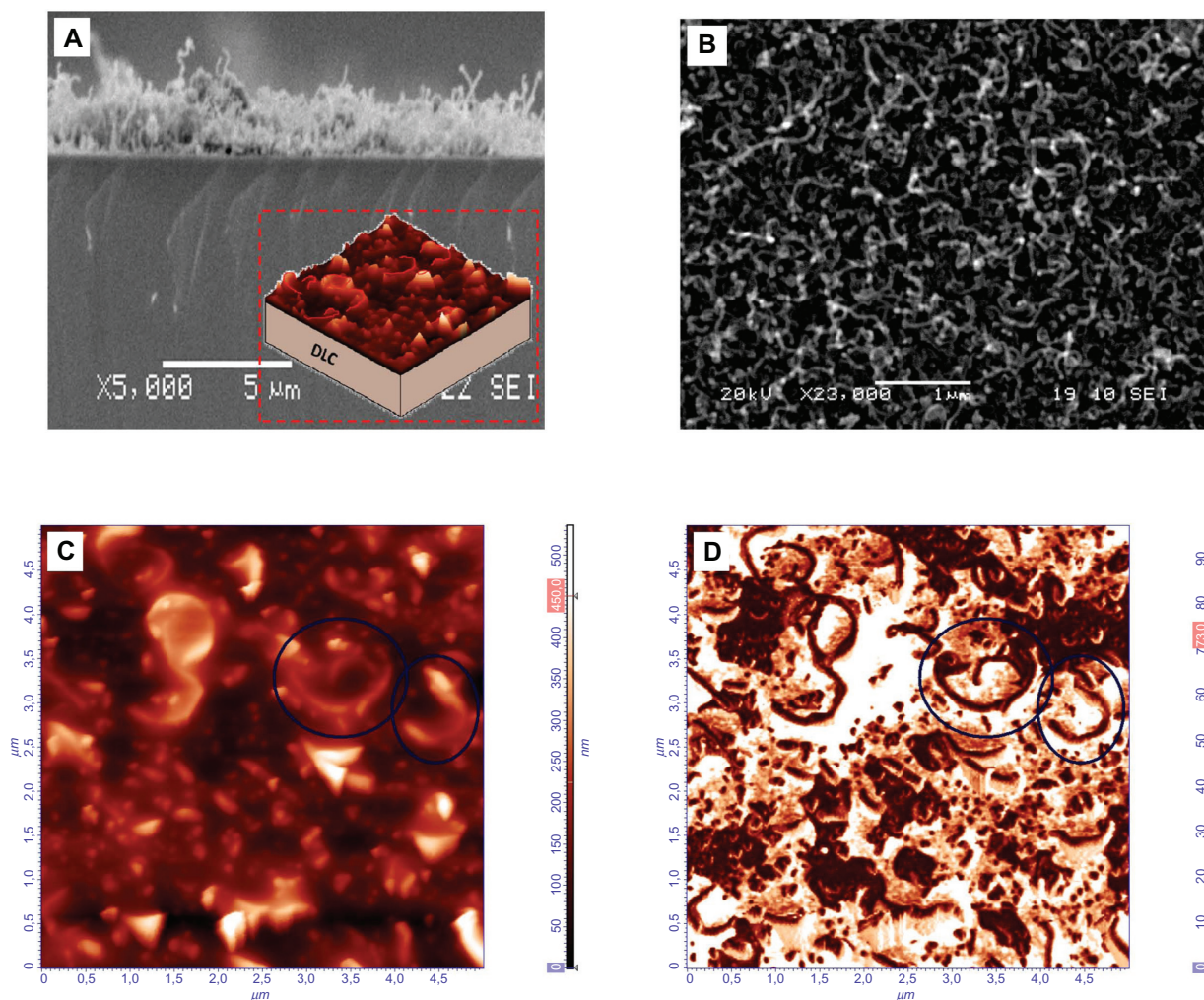
Figure 2 (**A**) Cross section of a scanning electron microscopy (SEM) image of carbon nanotubes (CNTs) on the diamond-like carbon (DLC) substrate (inset depicts a cartoon schematic detailing the CNTs deposited onto the DLC substrate). (**B**) SEM image showing the spaghetti-like structure of the CNTs. (**C**) Atomic force microscopy (AFM) topography image of the CNTs (circled), with spaghetti-like formation. (**D**) AFM phase image of the same CNTs shown in (**C**) the high contrast is indicative of nanopores.

investigated by AFM. The advantages of AFM over more conventional approaches such as SEM for platelet visualization are related to its atomic-scale resolution along the Z axis; real-time and three-dimensional imaging; non-destruction of the biological samples by the implementation of different AFM modes; no requirement for special preparation of the cells or vacuum conditions that would lead to cellular destruction; and, finally, ability to obtain informative image cross sections.[17]

Analysis of the AFM images was based on knowledge concerning the platelet morphological changes due to activation. Platelet shape changes followed a reproducible temporal sequence. The cells in their resting form are disc shaped, having a width of 0.5–3 µm and height of 120–200 nm. During activation, a cascade of events is triggered leading to the structural alteration of the cells: spherical shape, extension of finger-like projections from the cell periphery, flattening of the cells onto the surface, extension of broad lamellae and formation of pseudonucleus (with a fried-egg appearance) due to the accumulation of the dense and alpha granules into the centre, and elaboration of unique blunt filopodia from cellular periphery based on new cytoplasmic actin filaments.[18] It should be mentioned that the long, thin filopodia contain bundles of F-actin and the flat lamellae contained an orthogonal array of short filaments.[18] Simultaneously, the activated platelets release a few chemical compounds from their granules that can induce further activation of other platelets. The next step is the platelet aggregation, an essential procedure for thrombus formation.[19]

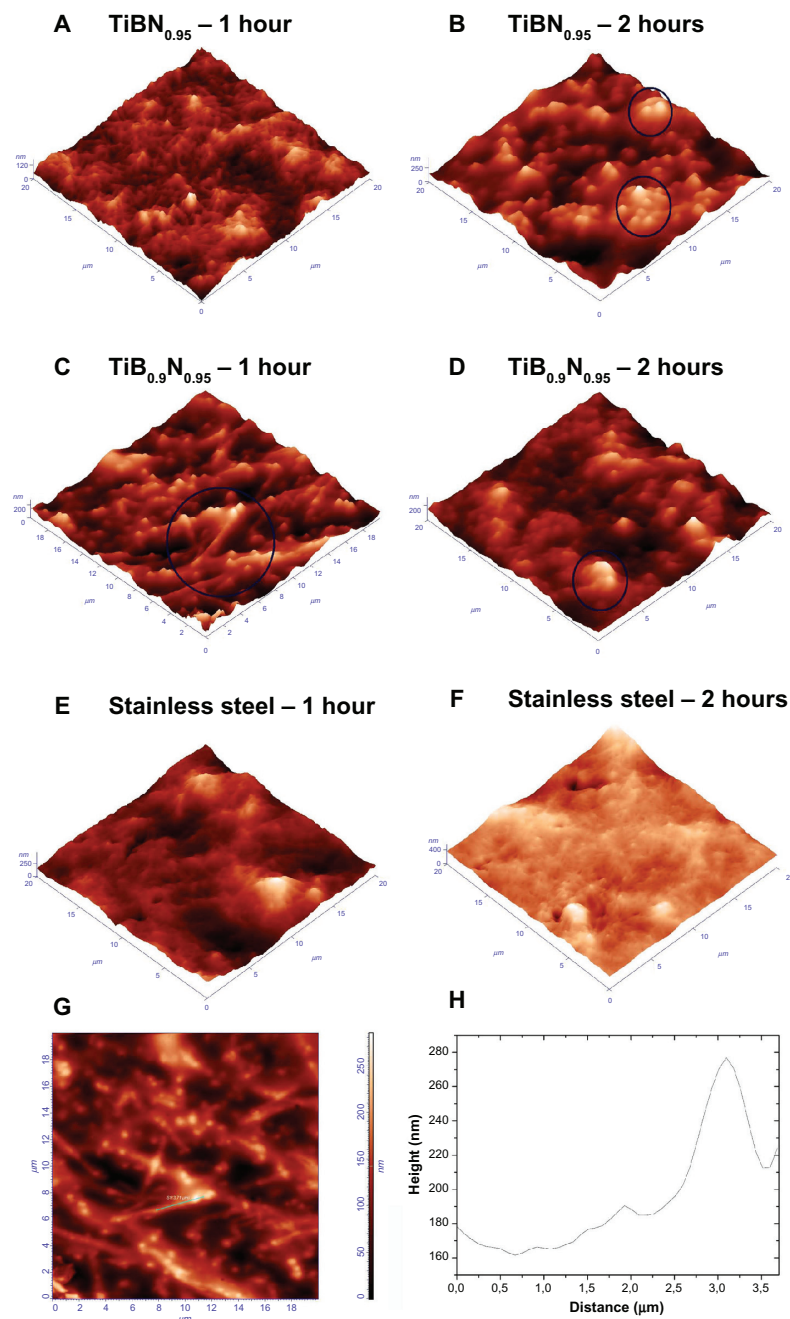## AFM studies of platelets on TiBN thin films and SS

Figures 3A and B depict the three-dimensional AFM topographic images of platelets adhered on $TiBN_{0.95}$ after 1 and 2 hours, respectively. After 1 hour of adhesion, the platelets underwent activation, as highlighted by the pseudonuclei and formation of a few pseudopodia; whereas, after 2 hours, the cells formed aggregates (of a maximum of two cells) with an approximate height of 250 nm (as denoted by the circles). By observing the AFM images of platelets adhering onto the $TiB_{0.9}N_{0.95}$ thin films, it was apparent that after 1 hour, the encircled platelets formed pseudonuclei with distinct pseudopodia (Figure 3C), and after 2 hours, an aggregation of two platelets was formed with the height of 200 nm (Figure 3D). In comparison, after 1 hour, the platelets on SS formed pseudonuclei with pseudopodia (Figure 3E) and, after 2 hours, they aggregated (the height of clusters measured approximately 400 nm [Figure 3F]).

It is of great importance to distinguish fibrin network from platelet pseudopodia when observing the AFM images of platelets adhering onto the samples. As platelet pseudopodia are cell membrane based, their continuity with cytoplasm is their main distinguishing feature. To ensure that the linear structures circled in Figure 3C were platelet pseudopodia and not fibrin networks, an appropriate cross section of the corresponding two-dimensional image was taken (Figure 3G and E).

Concerning the $TiB_{2.13}$ nanocoatings, the platelets developed pseudopodia and formed a network even from the first hour of adherence onto the substrate (Figure 4A). After 2 hours, on the same material, the platelet network prevailed, starting to form a thrombus (Figure 4B). AFM is a tool with versatile modes and allows detailed real-time imaging. For example, the cross-section profile along the marked horizontal line in Figure 4C (which depicts platelets on $TiB_{2.13}$ thin films) provided information about the platelet dimensions on activation. An activated platelet with pseudopodia, denoted by the circle, had a height of around 100 nm and width of about 2 µm. To comprehend the differences between the AFM imaging of platelets onto material interfaces and conventional imaging techniques like SEM, Figure 4D and E presents the SEM images of a platelet at an early stage of activation (showing a lack of discoid shape), followed by the development of filopodia at a higher degree of activation. Control experiments in which PRP was imaged on mica were performed and the AFM image of platelets onto mica after incubation for 2 hours is presented in Figure 4F. The AFM image of one activated platelet (scan size 5×5 µm) and the corresponding cross section along its filopodium are depicted in Figure 4G and H, respectively. As the pseudopodia are temporary cytoplasm-filled projections of the cell wall, their continuity with the cytoplasm, evident in Figure 4G and H, enabled them to be distinguished from the fibrin fibrils.

AFM studies of platelets on CNT/DLC and a-C:H thin films

The AFM topography images of platelets on the CNT/DLC coatings after 1 and 2 hours of observation are shown in Figure 5A and B, respectively. After 1 hour, platelets were at an early stage of activation, as apparant from their pseudonuclei (in white), and after 2 hours they did not form a network. Figure 5C is an AFM topography image of platelets on CNT/DLC thin films after 1 hour of incubation and its cross-section profile along the marked horizontal line. Herein, we observes a nanopore with a depth of approximately 150 nm.

A   TiBN$_{0.95}$ – 1 hour

B   TiBN$_{0.95}$ – 2 hours

C   TiB$_{0.9}$N$_{0.95}$ – 1 hour

D   TiB$_{0.9}$N$_{0.95}$ – 2 hours

E   Stainless steel – 1 hour

F   Stainless steel – 2 hours

G

H

Figure 3 Atomic force microscopy topography images of: (**A**) platelets on titanium (Ti) boron (B) nitride (N)$_{0.95}$ film after 1 hour of incubation time (scan size 20×20 µm); (**B**) platelets on TiBN$_{0.95}$ film after 2 hours of incubation, with a size of 20×20 µm (three-dimensional images) – circles indicate the formation of platelet aggregation; (**C**) platelets on TiB$_{0.9}$N$_{0.95}$ film after 1 hour of incubation; (**D**) platelets on TiB$_{0.9}$N$_{0.95}$ film after 2 hours of incubation time; (**E**) platelets on stainless steel, as control material, after 1 hour of cell adhesion; (**F**) platelets on stainless steel after 2 hours of incubation; (**G**) platelets on TiB$_{0.9}$N$_{0.95}$ film after 1 hour of incubation, corresponding to (**C**) (two-dimensional image). (**H**) Arbitrary cross section of image shown in (**G**).

Following this, we compared the aforementioned classes of biomaterials (TiBN, TiB$_2$, CNT/DLC, and SS) with types of a-C:H thin films that have been described in detail in our previous works.[20–22] After 2 hours' observation of platelets on a-C:H floating carbon thin films with a low hydrogen content in plasma during deposition (Figure 5D), it was noticed that the platelets did not aggregate; whereas, on biased carbon films, after the same time interval, the platelets made clusters that looked like islands (Figure 5E). These qualitative AFM data of the platelet behavior towards the examined biomaterials were presented quantitatively as R$_{rms}$ measurements of the examined nanomaterials, after 0, 1 hour, 1.5 hours, and 2 hours of platelet adhesion (Figure 6A) ($P < 0.001$).
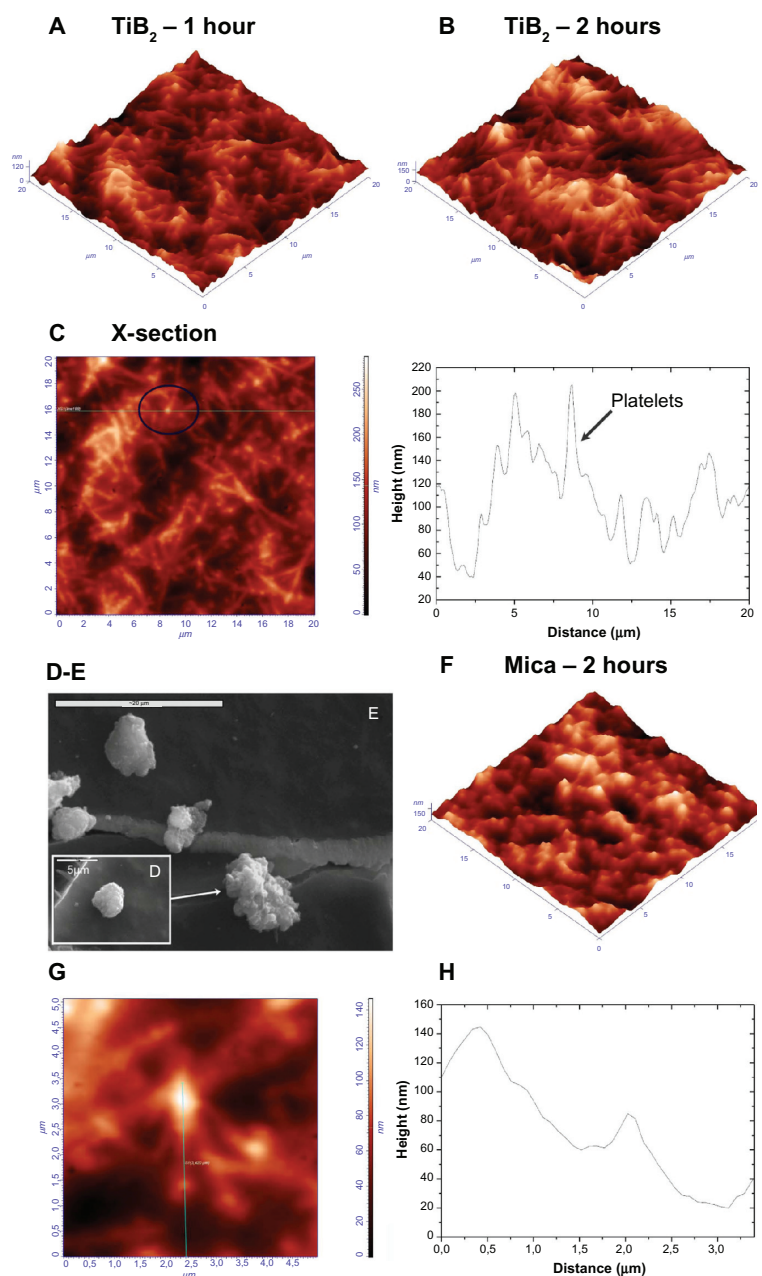
Figure 4 Atomic force microscopy (AFM) topography images of platelets on titanium (Ti) boron (B)$_{2.13}$ thin films: (**A**) after 1 hour of incubation, the cells developed pseudopodia and formed a network; (**B**) after 2 hours of incubation, platelet aggregation prevailed; (**C**) cross section at 16.9 μm, marked with the black circle, an activated platelet with pseudopodia (left) and, marked with the lines, the platelet and plasma protein aggregated on TiB$_{2.13}$ thin films (right); (**D**) scanning electron microscopy (SEM) image of a platelet at an early stage of activation; (**E**) SEM image of activated platelets that have lost their discoid shape and begun to develop pseudopodia; (**F**) AFM image of platelets obtained on mica after incubation for 2 hours (as control); (**G**) AFM image of activated platelets with filopodia (scan size of 5 × 5 μm). (**H**) Arbitrary cross section of an activated platelet along its pseudopodium.

Cell viability assay

Figure 7 shows the cell viability of the different groups of thin films. The best cytocompatibilty behavior was exhibited by TiB$_{0.9}$N$_{0.95}$ (TiBN_2) and the floating a-C:H thin films. CNT films in direct contact with the murine fibroblasts showed lower cell viability compared with the control group (only cells). The biased a-C:H thin films were the least cytocompatible thin fil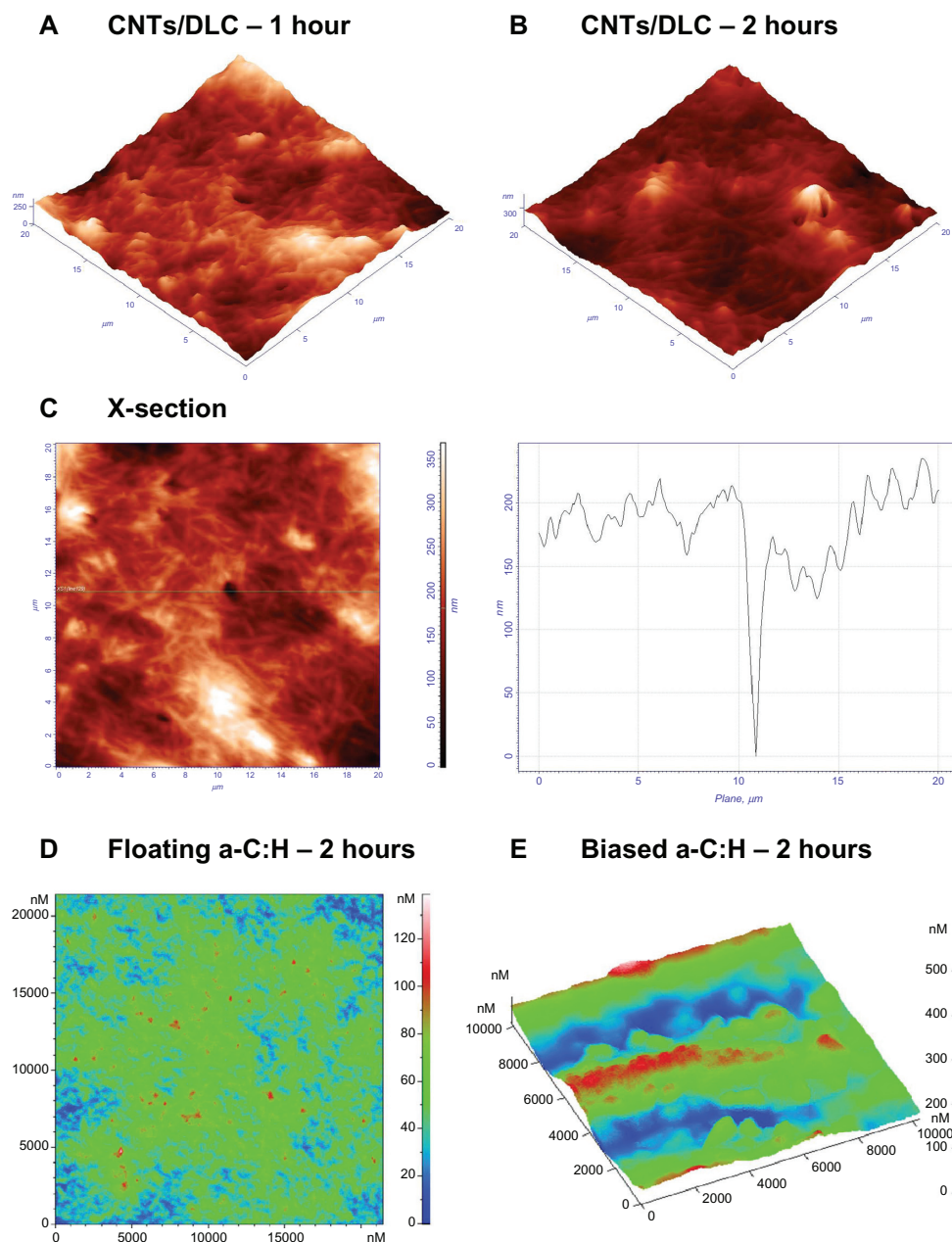ms. The cytotoxicity results were in full agreement with the data derived from the thrombogenicity evaluation of the engineered nanomaterials.

Discussion
Nanotechnology advances in cardiovascular implants

A wide range of vascular prosthetic devices, from stents to artificial heart valves and ventricular assisted devices, have
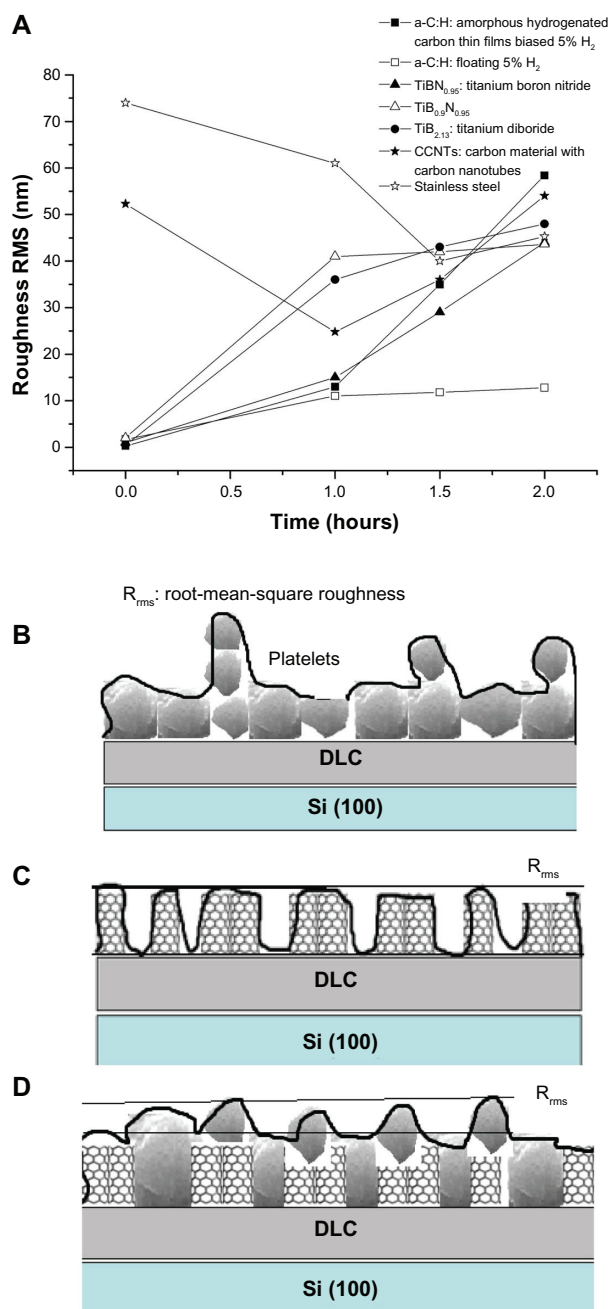
Figure 5 Atomic force microscopy (AFM) topography images of platelets onto: (**A**) carbon nanotube (CNT)/diamond-like carbon (DLC) coatings after 1 hour of incubation; (**B**) CNT/DLC coatings after 2 hours of incubation, and (**C**) 2D AFM image of CNT/DLC coatings after 1 hour of incubation (left) and a x-cross section profile at 12 μm showing a nanopore with a depth of 150nm (right). (**D**) Amorphous hydrogenated carbon (a-C:H) floating carbon thin films after 2 hours and (**E**) a-C:H-biased carbon thin films after 2 hours of adhesion, during which the platelets aggregated.

been implanted worldwide to treat patients that are often expected to live for many years after the procedures. As biomaterials promote surface-induced thrombotic phenomena to some extent, it is essential to evaluate their thrombogenicity. The study of thrombogenetic sequence originates from the platelet response to endothelium damage.

Limited knowledge about the interface phenomena on the border of living and nonliving matter, such as protein adsorption and platelet adhesion, are the theoretical foundation for the

attempt to develop biocompatible materials. The mechanisms of platelet adhesion constitute key questions in many studies, but despite the enormous research efforts, they are not yet fully understood. When this is translated into the development of coatings for stents, the elucidation of such mechanisms is necessary to deal with stent drawbacks.[23] The elucidation of such mechanisms can be seen as very necessary.

A wide variety of surface modifications and growth of inorganic stent coatings has been explored, targeting a range

A

Legend:
- a-C:H: amorphous hydrogenated carbon thin films biased 5% H_2
- a-C:H: floating 5% H_2
- $TiBN_{0.95}$: titanium boron nitride
- $TiB_{0.9}N_{0.95}$
- $TiB_{2.13}$: titanium diboride
- CCNTs: carbon material with carbon nanotubes
- Stainless steel

B

R_{rms}: root-mean-square roughness

Platelets

DLC

Si (100)

C

R_{rms}

DLC

Si (100)

D

R_{rms}

DLC

Si (100)

Figure 6 (**A**) Comparative diagram showing the root-mean-square roughness (R_{rms}) values of the engineered nanomaterials, after 0, 1 hour, 1.5 hours, and 2 hours of platelet adhesion. (**B**) Schematic illustration of a time-dependent increase in surface roughness (R_{rms}) depending on platelet adhesion onto bare carbon and titanium thin films of low nanoroughness. Schematic representations of (**C**) an increase in R_{rms} on bare carbon nanotube (CNT)/diamond-like carbon (DLC) nanocoatings due to CNT bundles and (**D**) a decrease in R_{rms} during platelet aggregation on the CNT/DLC substrates.

of objectives such as reduced metal ion release, avoidance of surface thrombogenicity, and texturing to promote endothelialization.[24] Nanotechnology provides material manufacturers with the ability to fabricate and control material properties. After decreasing the size of materials to the nanoscale, a dramatically increased surface area and surface area to volume ratio are produced that can lead to superior physical properties (ie, mechanical, electrical, and optical, etc). Nanomaterials with such excellent properties have been extensively investigated in a wide range of biomedical applications, such as vascular stents.[25] This research has been fostered by the facts that the vascular walls possess numerous nanostructured features (eg, due to the presence of collagen and elastin in the vascular endothelial cellular matrix) and that nanomaterials mimic the endothelium structure. Choudhary et al reported that vascular cell adhesion and proliferation were greatly improved on nanostructured titanium compared with conventional titanium.[25] The nanotechnology strategies deal not only with the enhancement of stent endothelialization but also with the avoidance of stent thrombosis. Much research demonstrates the thrombogenicity assessment of various classes of nanomaterials. For example, Maguire et al reported the reduced thrombogenicity of amorphous DLC materials for stents and medical guide wires.[26]

Nanomaterial properties dictate platelet response

This study focused on the influence of surface nanotopography and physicochemical characteristics of carbon- and titanium-based biomaterials on cell viability and, especially, on platelet structural changes, as an index of activation. Thrombogenic assessment of the examined materials will lead to the selection of those that are more thromboprotective and thus may be used as an additional layer to coat the existing stent metal platforms. The ultimate goal is to reduce stent thrombosis.

It is well described that implanted materials are immediately coated with proteins from blood and interstitial fluids, and it is through this adsorbed layer that cells sense foreign surfaces. In previous studies, we have developed a methodology to study the possibility of thrombus formation during material–protein interactions, the optical properties of the adsorbed plasma proteins, and their adsorption mechanisms.[10,14] Ex-situ spectroscopic ellipsometry measurements in the energy region of 1.5–6.5 eV of human albumin and fibrinogen adsorbed onto a-C:H thin films and AFM studies have shown that the carbon hybridization, configuration, and hydrogen content determine surface properties, protein adsorption, and platelet behavior.[9,10,27] The sp^3 fractions of the engineered a-C:H thin films in the present study were about 40%–44%, which has been found to be the optimum value in terms of the hemocompatibility of carbon-based thin films (Logothetidis et al[14]). In this study, the low content of hydrogen in plasma and the absence of ion
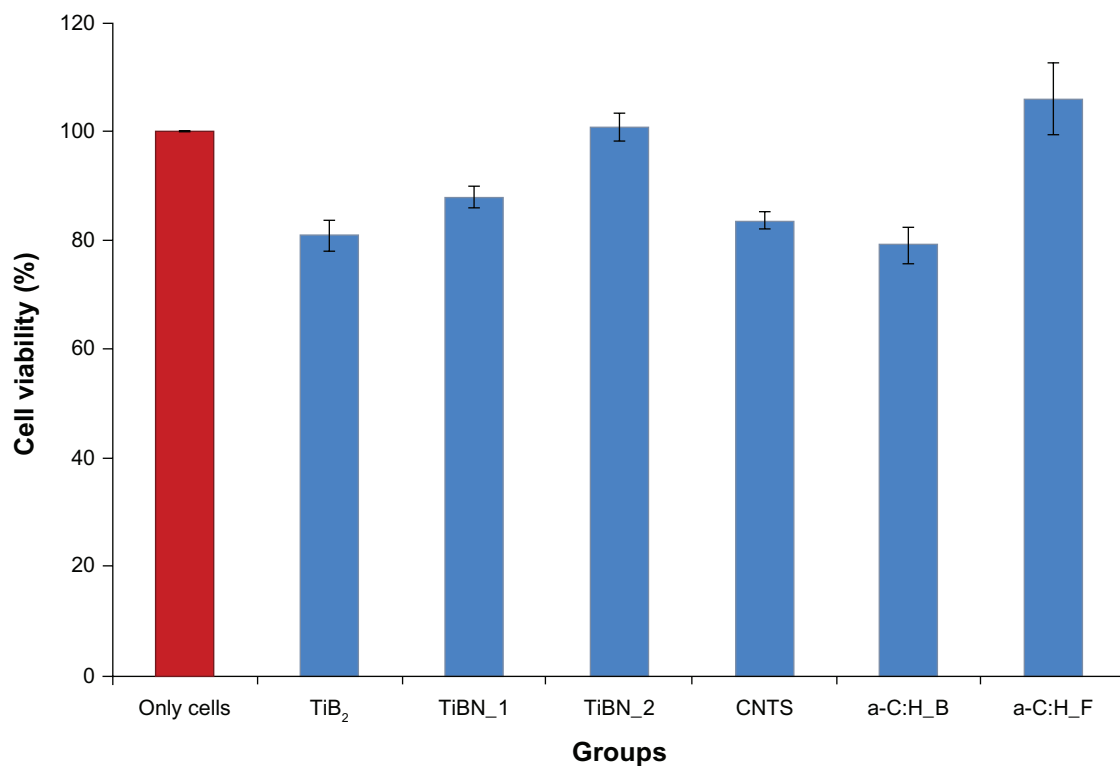
Figure 7 Comparative diagram showing the L929 fibroblasts viability in direct contact with the engineered materials for 24 hours under static conditions.
Abbreviations: a-C:H, amorphous hydrogenated carbon thin films; a-C:H_B, biased amorphous hydrogenated carbon thin films; a-C:H_F, floating amorphous hydrogenated carbon thin films; TiBN, titanium boron nitride; TiBN_I, $TiBN_{0.95}$; TiBN_2, $TiB_{0.9}N_{0.95}$; TiB_2, titanium diboride; CNTs, carbon nanomaterial with carbon nanotubes; MTT, 3-(4,5-Dimethylthiazol-2-yl)-2,5-diphenyltetrazolium bromide.

bombardment during deposition of the carbon films lead to surface nanotopography that repelled platelets. The surface nanoroughness of the floating a-C:H thin film of approximately 2 nm was found to influence platelet response. In contrast, the atomically smoother a-C:H films (biased) were found to be more thrombogenic and less cytocompatible. These slight variations in the surface roughness of the two types of carbon materials are to be expected, as in vivo cells respond to textured cues in the extracellular matrix that contain pores, protrusions, pits, and fibers in the length scale of 5–200 nm.[28]

Upon adhesion to a substrate, the cell probes its environment and moves using nanometer-scale structures such as filopodia and lamellipodia. Filopodia probe the environment around the cell and their ends serve as anchor points for movement.[29] As these structures have sizes in the nanometer range (eg, platelet filopodia have a tip diameter of 120 nm, as measured by AFM[9]), it is likely that they will be influenced by nanotopography. These observations can also be explained by the fact that the nature of the biomaterial surface is a significant factor in the protein adsorption that mediates platelet interactions. It is fully accepted that the presence of proteins adsorbed on the artificial surface play a crucial role in mediat-

ing the initial interactions of platelets with the surface, and the composition of the synthetic surface is a key determinant in the rate and nature of the protein adsorbed.[30] Our previous studies have shown that human albumin is adsorbed more easily on floating carbon thin films with nanoroughness and a low hydrogen content in plasma. In contrast, fibrinogen is favorably adsorbed into biased carbon coatings in comparison to floating ones.[8] The electrical properties of the carbon thin films have been found to strongly affect the reactions of the electrically negative platelets.[31]

The TiBN films have a large number of uses in the cutting and decorative applications.[32] They exhibit low corrosion current density in acid environments, high oxidation resistance, and excellent abrasive wear resistance accompanied with high thermal stability.[33] The lack of studies on their biomedical use gave us the stimulus for their thrombogenicity analysis. The biased TiBN films were found to possess better biological properties compared with biased carbon films. Although the biased TiBN and carbon films are ultra smooth, due to their layer-by-layer growth, it can be noted that in these classes of materials, the stoichiometry is more important than the nanotopography. It is known that the surface chemistry on the nanometer scale can be a deciding factor

in the recruitment of specific cell membrane integrins acting as cell attachment molecules. Upon attachment to a surface, the integrin receptors cluster together and recruit cytoplasmic proteins to form the focal contacts.[29] In the case of platelets, glycoprotein IIb/IIIa (also known as integrin α2bβ3) interacts with the amino acid sequence arginyl-glycyl-aspartyl-serine (RGDS) present on several adhesive proteins (fibrinogen, von Willebrand factor, and fibronectin) and the glycoprotein Ib-IX complex interacts with the insoluble von Willebrand factor bound to the subendothelium.[19]

The AFM studies revealed that when the nitrogen content of the TiBN films increases, their thrombogenicity is reduced while their cytocompatibility increases in comparison with the control material. This can be justified partially by the albumin adsorption that is enhanced on these surfaces.[34] The addition of nitrogen into the coating is an interesting aspect that has not been widely addressed. Endothelium-derived nitric oxide is known to be important in regulating endothelial function, helping suppress platelet aggregation, and cellular adhesion to the endothelium, and even in inhibiting smooth muscle cell proliferation. A titanium-nitride oxide coating has been developed for stent applications and its effects are promising.[35]

Due to their specific structure/texture and properties, CNTs are emerging materials that may play a significant role in the development of carbon materials for medicine.[36] However, it must be noted that the biocompatibility of CNTs is still in question and is being actively studied by different research groups.[37,38] In our study, it was found that coatings composed of CNTs exhibit less hemocompatibility than both TiBN and the reference material. The AFM images showed nanostructures on the surface of the CNTs based coatings attributed to the presence of CNTs and nanopores due to the special preparation of the films. As the cells are able to respond to nanostructures, these surface irregularities may have a significant impact on the organization of focal adhesions formed in platelets, either by disrupting their elongation or by inducing specific integrin recruitment.[29] The changes in platelet morphology, such as stretching on the nanogrooves between the CNTs, can result in differential stress that is not present when the cell is grown on a flat surface. This mechano-transduction process can transmit information from outside into the cell and can induce changes in cell behavior.

The high nanoroughness of the CNT/DLC thin films, which reaches 52 nm, is not favorable to the inhibition of platelet aggregation. This finding is in agreement with data from a study on the influence of surface roughness on the activation of coagulation and platelet adhesion on continuous flow blood pumps.[39] In their study, Linneweber et al showed that surface roughness greater than 50 nm stimulates platelet adhesion and fibrinogen adsorption, indicating a reduction in anti-thrombogenicity in devices with rougher metal finishes.[39]

What is remarkable is the fact that both carbon- (without nanotubes) and titanium-based films showed a time-dependant increase in surface roughness (R_{rms}) depending on platelet adhesion and aggregation onto the substrates. In contrast, the bare CNT/DLC nanocoatings had high R_{rms} values due to the CNT bundles, but this then decreased because of the platelet adhesion during time. A schematic illustration of this phenomenon is depicted in Figure 6B–D. Following the same trend, the roughness of the SS material was reduced, owing to platelet aggregation, after 1.5 hours of AFM observation and then, within 2 hours, it increased slightly again.

The correlation between surface wettability and thrombogenicity has been confirmed by several studies.[40,41] The wettability measurements in the present study show that the surface free energy of the materials and their hydrophilicity/hydrophobicity dictate platelet response. The CNT/DLC and TiBN thin films were found to be hydrophobic, whereas the CAs of the a-C:H and TiB_2 samples indicated their hydrophilic nature. The CNTs/DLC films were more hydrophobic in comparison with the TiBN thin films. No statistical difference between the measured CAs of the TiBN classes was found, and there was no obvious effect of this on the thrombogenicity properties. In these materials, surface chemistry seems to play a key role in platelet behavior. The good hemocompatible behavior of the a-C:H materials can be partially attributed to their hydrophilicity, as most hydrophilic films exhibited a better protein to surface concentration ratio.[34] The surface of the floating a-C:H thin films may mimic the properties of endothelial cells lining blood vessels, which have a net negative charge and are also hydrophilic. These two properties have been postulated to decrease the attachment of platelets.[41] Overall, the surface chemistry, nanotopographical features, and wetting properties of the examined materials influence the variability of platelet response when they come into contact.

Hence, cell activation and motility are ultimately mechanical phenomena, but little is known about the mechanical and physical properties of moving cells.[42] A few AFM studies of time-dependent structural changes, cell migration, and the associated changes in mechanical properties have been reported for platelets.[43] Fritz et al[43] demonstrated that platelets

that have bound to the surface but remain inactivated can be scanned by AFM at low forces with no noticeable time-dependent changes in shape. However, scanning at higher forces promotes their activation. Radmacher et al[44] reported that the elastic modulus values of activated platelets were in the range of 1–50 kPa, as measured by force mapping techniques. Further, a recent study shown that platelet contraction reaches a steady state after 25 minutes, displaying total forces of ~34 nN.[45]

Taking into account the mechanical aspects of cell motility, a limitation of the present study is that the platelet experiments were performed under in vitro conditions without the influence of blood flow and shear stress on platelet activation. Moreover, in humans, the complex coagulation system and the interplay between the plasma proteins and blood cells with the vascular biomaterials result in difficulties in comprehending their biocompatibility. Future studies will address this issue to enhance our knowledge about how platelets interact with stent nanomaterials in atherosclerotic human arteries.

Conclusion

This work presents strong evidence that the surface chemistry, nanostructure, and wetting properties are the parameters that greatly determine platelet adhesion and the cytocompatibility behavior of a surface. In this work, a range of nanomaterials, ranging from a:C:H and CNT/DLC thin films to TiBN and TiB_2 thin films was developed, characterized, and studied for potential application as stent coatings.

The carbon hybridization, hydrogen content, and configuration of carbon films (grown by sputtering technique) were found to determine their physicochemical and biological properties. The low content of hydrogen in plasma and the absence of ion bombardment during deposition of the carbon films led to surface nanotopography that inhibited platelet aggregation. Their hydrophilic nature and slight nanoroughness favorably influenced platelet behavior. In contrast, the atomically smooth carbon nanocoatings (biased) had the opposite effect.

The surface chemistry of the TiBN thin films, especially the higher nitrogen content, dictated the inhibition of clot formation. The AFM results indicated that the biased TiBN films were less thrombogenic compared with biased carbon films. CNT coatings, as grown by chemical vapor deposition, were found to be less hemocompatible than the controls. Their high nanoroughness due to CNT bundles and hydrophobicity played a significant role in their low thromboprotectivity. The nanomaterials exhibited strong differences in terms of

wettability. The surface free energy affected the thrombogenic properties, since good hemocompatible behavior was observed in the materials with higher surface free energy, such as the a-C:H films.

Overall, the results indicate that nanostructure modifications, stoichiometry, and hydrophilicity of biomaterial surfaces could elicit the desired platelet response and cytocompatibility, which could be significant in the development of blood-contacting materials like stent coatings.

Acknowledgment

Disclosure

The authors declare no conflicts of interest in this work.

References

1. Colombo A, Iakovou I. Drug-eluting stents: the new gold standard for percutaneous coronary revascularisation. *Eur Heart J*. 2004;25(11): 895–897.
2. Smith EJ, Jain KA, Rothman MT. New developments in coronary stent technology. *J Interv Cardiol*. 2006;19(6):493–499.
3. Stone GW, Moses JW, Ellis SG, et al. Safety and efficacy of sirolimus- and paclitaxel-eluting coronary stents. *N Engl J Med*. 2007;356(10):998–1008.
4. Bavry AA, Kumbhani DJ, Helton TJ, Borek PP, Mood GR, Bhatt DL. Late thrombosis of drug-eluting stents: a meta-analysis of randomized clinical trials. *Am J Med*. 2006;119(12):1056–1061.
5. Hara H, Nakamura M, Palmaz JC, Schwartz RS. Role of stent design and coatings on restenosis and thrombosis. *Adv Drug Deliv Rev*. 2006;58(3):377–386.
6. Zhang L, Webster TJ. Nanotechnology and nanomaterials: promises for improved tissue regeneration. *Nano Today*. 2009;4(1):66–80.
7. Nakano K, Egashira K, Masuda S, et al. Formulation of nanoparticle-eluting stents by a cationic electrodeposition coating technology: efficient nano-drug delivery via bioabsorbable polymeric nanoparticle-eluting stents in porcine coronary arteries. *JACC Cardiovasc Interv*. 2009;2(4):277–283.
8. Logothetidis S. Haemocompatibility of carbon based thin films. *Diam Relat Mater*. 2007;16(10):1847–1857.
9. Karagkiozaki VC, Logothetidis SD, Kassavetis SN, Giannoglou GD. Nanomedicine for the reduction of the thrombogenicity of stent coatings. *Int J Nanomedicine*. 2010;5:239–248.
10. Lousinian S, Logothetidis S, Laskarakis A, Gioti M. Haemocompatibility of amorphous hydrogenated carbon thin films, optical properties and adsorption mechanisms of blood plasma proteins. *Biomol Eng*. 2007;24(1):107–112.
11. García-González L, Hernández-Torres J, García-Ramírez PJ, et al. Structure and mechanical properties of TiBN coatings fabricated by dc reactive sputtering technique. *J Mater Process Technol*. 2007;186(1–3): 362–366.
12. Yang Z, Zhang Y, Yang Y, et al. Pharmacological and toxicological target organelles and safe use of single-walled carbon nanotubes as drug carriers in treating Alzheimer disease. *Nanomedicine*. 2010;6(3): 427–441.
13. Ménard-Moyon C, Kostarelos K, Prato M, Bianco A. Functionalized carbon nanotubes for probing and modulating molecular functions. *J Chem Biol*. 2010;17(2):107–115.

14. Logothetidis S, Gioti M, Lousinian S, Fotiadou S. Haemocompatibility studies on carbon-based thin films by ellipsometry. *Thin Solid Films*. 2005;482(1–2):126–132.

15. Chibowski E, Perea-Carpio R. Problems of contact angle and solid surface free energy determination. *Adv Colloid Interface Sci*. 2002;98(2):245–264.

16. Müller DJ, Anderson K. Biomolecular imaging using atomic force microscopy. *Trends Biotechnol*. 2002;20(8):S45–S49.

17. Allison DP, Mortensen NP, Sullivan CJ, Doktycz MJ. Atomic force microscopy of biological samples. *Wiley Interdisc Rev Nanomed Nanobiotechnol*. 2010;2(6):618–634.

18. Karagkiozaki V, Logothetidis S, Kalfagiannis N, Lousinian S, Giannoglou G. Atomic force microscopy probing platelet activation behavior on titanium nitride nanocoatings for biomedical applications. *Nanomedicine*. 2009;5(1):64–72.

19. Hartwig JH. Platelet structure. In: Michelson AD, editor. *Platelets*. San Diego, CA: Academic Press; 2002:37–45.

20. Karagkiozaki V, Logothetidis S, Giannoglou G. Advances in stent coating technology via nanotechnology tools and process. *Eur J Nanomed*. 2008;1(1):24–28.

21. Karagkiozaki V, Logothetidis S, Kassavetis S, Lousinian S. Nanoscale characterization of biological and mechanical profile of carbon stent nanocoatings. *Eur J Nanomed*. 2009;2(1):14–21.

22. Karagkiozaki V, Logothetidis S, Laskarakis A, Giannoglou G, Lousinian S. AFM study of the thrombogenicity of carbon-based coatings for cardiovascular applications. *Mater Sci Eng B*. 2008;152(1–3):16–21.

23. Joner M, Finn AV, Farb A, et al. Pathology of drug-eluting stents in humans: delayed healing and late thrombotic risk. *J Am Coll Cardiol*. 2006;48(1):193–202.

24. O'Brien B, Carroll W. The evolution of cardiovascular stent materials and surfaces in response to clinical drivers: a review. *Acta Biomater*. 2009;5(4):945–958.

25. Choudhary S, Berhe M, Haberstroh KM, Webster TJ. Increased endothelial and vascular smooth muscle cell adhesion on nanostructured titanium and CoCrMo. *Int J Nanomed*. 2006;1(1):41–49.

26. Maguire PD, McLaughlin JA, Okpalugo TI, et al. Mechanical stability, corrosion performance and bioresponse of amorphous diamond-like carbon for medical stents and guidewires. *Diam Relat Mater*. 2005;14(8):1277–1288.

27. Mitsakakis K, Lousinian S, Logothetidis S. Early stages of human plasma proteins adsorption probed by Atomic Force Microscope. *Biomol Eng*. 2007;24(1):119–124.

28. Lord MS, Foss M, Besenbacher F. Influence of nanoscale surface topography on protein adsorption and cellular response. *Nano Today*. 2010;5(1):66–78.

29. Anselme K, Davidson P, Popa AM, Giazzon M, Liley M, Ploux L. The interaction of cells and bacteria with surfaces structured at the nanometre scale. *Acta Biomater*. 2010;6(10):824–846.

30. Yang P, Huang N, Leng YX, et al. Activation of platelets adhered on amorphous hydrogenated carbon (a-C:H) films synthesized by plasma immersion ion implantation-deposition (PIII-D). *Biomaterials*. 2003;24(17):2821–2829.

31. Karagkiozaki V, Logothetidis S, Lousinian S, Giannoglou G. Impact of surface electric properties of carbon-based thin films on platelets activation for nano-medical and nano-sensing applications. *Int J Nanomed*. 2008;3(4):461–469.

32. Holzschuh H. Deposition of Ti–B–N (single and multilayer) and Zr–B–N coatings by chemical vapor deposition techniques on cutting tools. *Thin Solid Films*. 2004;469–470:92–98.

33. Aouadi SM, Debessai M, Namavar F, Wong KC, Mitchell KA. Titanium boron nitride films grown by ion beam assisted deposition: chemical and optical characterization. *Surf Coat Technol*. 2004;183(2–3):369–377.

34. Lousinian S, Kalfagiannis N, Logothetidis S. Albumin and fibrinogen adsorption on boron nitride and carbon-based thin films. *Mater Sci Eng B*. 2008;152(1–3):12–15.

35. Vallance P, Chan N. Endothelial function and nitric oxide: clinical relevance. *Heart*. 2001;85(3):342–350.

36. Usui Y, Aoki K, Narita N, et al. Carbon nanotubes with high bone-tissue compatibility and bone-formation acceleration effects. *Small*. 2008;4(2):240–246.

37. Kim JY, Khang D, Lee JE, Webster TJ. Decreased macrophage density on carbon nanotube patterns on polycarbonate urethane. *J Biomed Mater Res A*. 2009;8(2):419–426.

38. Muller J, Huaux F, Fonseca A, et al. Structural defects play a major role in the acute lung toxicity of multiwall carbon nanotubes: toxicological aspects. *Chem Res Toxicol*. 2008;21(9):1698–1705.

39. Linneweber J, Dohmen PM, Kertzscher U, Affeld K, Nosé Y, Konertz W. The effect of surface roughness on activation of the coagulation system and platelet adhesion in rotary blood pumps. *Artif Organs*. 2007;31(5):345–351.

40. Xu LC, Siedlecki CA. Effects of surface wettability and contact time on protein adhesion to biomaterial surfaces. *Biomaterials*. 2007;28(22):3273–3283.

41. Tulloch AW, Chun Y, Levi DS, et al. Super hydrophilic thin film nitinol demonstrates reduced platelet adhesion compared with commercially available endograft materials. *J Surg Res*. 2011;171(1):317–322.

42. Kuznetsova TG, Starodubtseva MN, Yegorenkov NI, Chizhik SA, Zhdanov RI. Atomic force microscopy probing of cell elasticity. *Micron*. 2007;38(8):824–833.

43. Fritz M, Radmacher M, Gaub HE. Granula motion and membrane spreading during activation of human platelets imaged by atomic force microscopy. *Biophys J*. 1994;66(5):1328–1334.

44. Radmacher M, Fritz M, Kacher M, Cleveland P, Hansma, K. Measuring the viscoelastic properties of human platelets with the atomic force microscope. *Biophys J*. 1996;70(1):556–567.

45. Henriques SS, Sandmann R, Strate A, Köster S. Force field evolution during human blood platelet activation. *J Cell Sci*. 2012. Epub May 11.